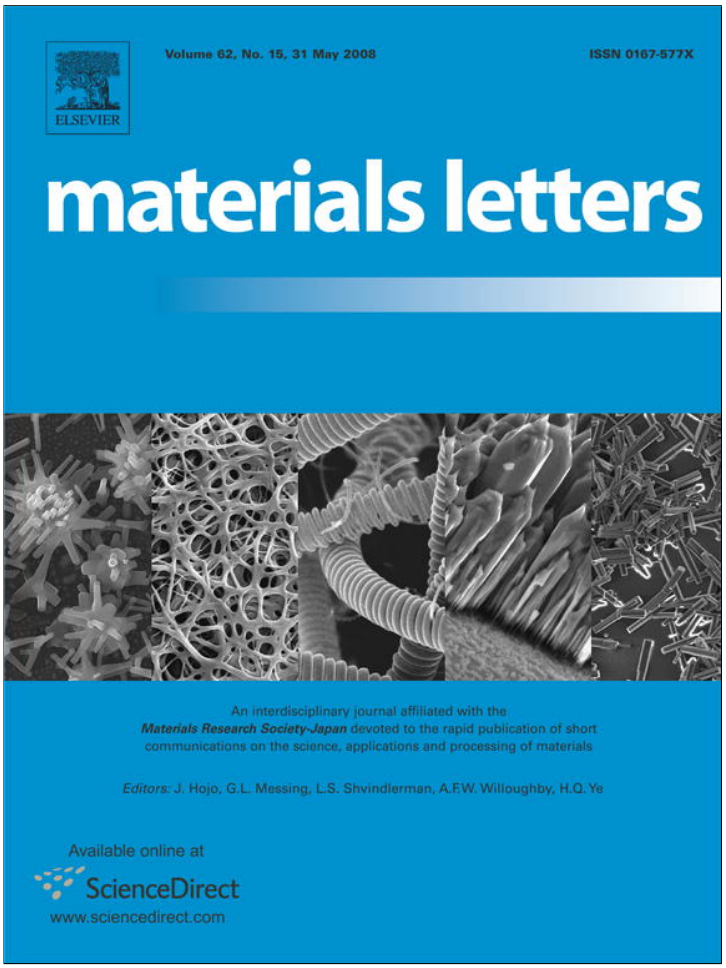

Available online at www.sciencedirect.com
ScienceDirect
Materials Letters 62 (2008) 2285–2288
materials letters
www.elsevier.com/locate/matlet

The growth of nickel nanoparticles on conductive polymer composite electrodes

N.F. Heinig [a], N. Kharbanda [a], M.R. Pynenburg [a], X.J. Zhou [a], G.A. Schultz [b], K.T. Leung [a,b,*]

[a] Department of Chemistry, University of Waterloo, Waterloo, Ontario, Canada, N2L 3G1
[b] Deparment of Physics, University of Waterloo, Waterloo, Ontario, Canada, N2L 3G1

Received 24 March 2007; accepted 23 November 2007
Available online 8 December 2007

Abstract

Uniformly sized and dispersed nickel core-shell nanoparticles on polypyrrole have been grown by electrodeposition. Two principal types of Ni particle morphologies were observed: small Ni nanocrystallites ranging in diameter from 7 to 12 nm, and larger spherical Ni clusters of 100 nm to over a micron in size. The type of Ni nanoparticles deposited depends sensitively on the preparation of the conducting polymer substrate. The optimal deposition conditions for the small Ni nanocrystallites were determined. TEM diffraction and XPS analysis show that these nanoparticles are predominantly NiO.

Keywords: Nanoparticles; Nanocrystallites; Electrodeposition; Conductive polymer composite

1. Introduction

Nanosized metal particles are interesting because their chemical and physical properties are often quite different from the corresponding bulk material. Nanoparticles dispersed onto electron-conducting polymers, such as polypyrrole (PPy), have many technological applications, especially in the areas of catalysis, chemical sensors, and electronic devices [1–4]. Nickel nanoparticles can be synthesized using solution chemistry [5,6], while cluster synthesis and deposition from the gas phase [2,4] have also been used successfully. Electrochemical deposition is an inexpensive and flexible synthesis method, and may provide better dispersion of the nanoparticles than these other techniques. Electrochemical deposition has already been found useful in producing Ni nanoparticles on graphite, ranging in diameter from 20 to 600 nm [1].

Recently, we studied the deposition of copper nanoparticles on thin PPy films electrodeposited onto gold-coated silicon electrodes [7]. By systematically varying such parameters as PPy thickness, applied potential, and electrolyte concentration, good control over the size, distribution and morphology of the copper nanocrystals was demonstrated [7,8]. In the present work, we apply these general strategies to deposit Ni nanoparticles onto PPy on gold-coated silicon electrodes. With careful control of the initial PPy film growth (particularly the current density), well-dispersed, near-spherical Ni nanoparticles with good size monodispersity in the range of 7 to 12 nm in diameter could be synthesized. To our knowledge, these particles represent the smallest Ni nanoparticles ever produced on an organic semiconductor substrate. With the dimension approaching the critical size limit that exhibits quantum size effects (<5 nm), the synthesis and characterization of these nanoparticles on a substrate are of special interest to applications in nanocatalysis and quantum electronics.

2. Experimental details

The Ni nanoparticles were grown on PPy films that were electrochemically deposited onto gold-coated silicon chips. The rectangular Si chips (10×2.5 mm^2) were cut from a n-type,

* Corresponding author. Department of Chemistry, University of Waterloo, Waterloo, Ontario, Canada, N2L 3G1. Fax: +1 519 746 0435.
E-mail address: tong@uwaterloo.ca (K.T. Leung).

0167-577X/$ - see front matter © 2007 Elsevier B.V. All rights reserved.
doi:10.1016/j.matlet.2007.11.094

Si(100) wafer with a resistivity of 1.0–1.5 mΩ·cm. A gold film of 80–100 nm thickness was sputter-deposited onto the silicon chip using a magnetron sputter-coater (Denton Desk II). The PPy films were grown galvanostatically from an aqueous solution of 0.05 M pyrrole and 0.1 M $NaClO_4$, after deoxygenation by bubbling nitrogen through the solution for 20 min. An Ag/AgCl reference electrode was used for all the electrochemistry experiments unless stated otherwise. The pyrrole stock solution was made-up anew as needed, or when a slight brown tint (indicative of the presence of oligimers) became visible. The PPy film thickness was estimated by measuring the total charge transferred during growth, and this thickness was confirmed by Atomic Force Microscopy (AFM) measurements. The PPy films were then rinsed thoroughly with deionized Millipore water (with a resistivity of 18.2 MΩ·cm), followed by drying. Nickel nanoparticles were deposited onto the PPy film (typically 100 nm thick) potentiostatically in a solution of 1×10^{-6} M H_2SO_4, 0.01 M H_3BO_3, and 0.01 M $NiSO_4{\cdot}6H_2O$ [18] by using amperometry, typically at −1.4 V (relative to the Ag/AgCl reference electrode) unless stated otherwise. Further experimental details were given in our earlier work [7].

The samples were characterized by using a LEO 1530 field-emission scanning electron microscopy (SEM) at an accelerating voltage of 5 kV. Selected samples were also characterized in a JEOL CM-20 transmission electron microscope (TEM) operating at 200 kV. The TEM specimens were prepared by mounting flakes of the Ni/PPy samples onto a copper grid. X-ray photoelectron spectroscopy (XPS) data was also collected by using a Thermo-VG Scientific ESCALab 250 Imaging Microprobe, with a typical energy resolution of 0.4–0.5 eV full-width at half-maximum.

3. Results and discussion

3.1. Polypyrrole growth

Initially, Ni nanoparticle growth on PPy was found to be less reproducible than that observed previously for copper nanoparticles on PPy [7,8]. This appears to be due to Ni growth being considerably more sensitive than copper to the properties of the PPy substrate. Nickel nanoparticle growth was also found to depend strongly on the selected current density during the PPy electrodeposition. Several papers have commented on the effects of the current density during electrodeposition on the microstructure of the electrodeposited PPy [9–11], and they suggested that lower current densities should lead to more uniform PPy films. In the present work, this point was further investigated by growing a large number of PPy films at a number of different current densities. For each film, the nominal PPy thickness was kept constant at 100 nm by adjusting the deposition time. Each voltage-time transient is displayed as a point in Fig. 1, where the voltage at the end of the PPy deposition is plotted against the applied anodic current density. While the end-point voltage increases gradually from 0.5 to 0.8 V as the anodic current density increases, there is a very sharp transition marked by a sudden increase in the end-point voltage to ~2 V at an anodic current density of 15–20 mA/cm^2. The scatter seen in Fig. 1 can be attributed to the aging of the pyrrole solution. In particular, freshly distilled pyrrole and newly made-up stock solutions tended to have a 2 V end-point transition at higher anodic current densities than older pyrrole solutions.

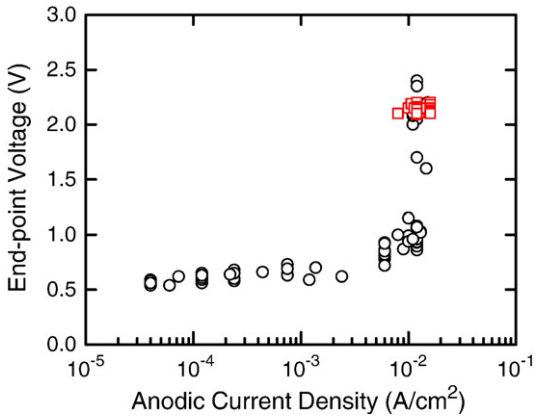

Fig. 1. End-point voltage as a function of anodic current density, collected during electrodeposition, for a number of polypyrrole films. The squares and circles correspond to two data sets (collected at different times) with average substrate sizes of 0.15 cm^2 and 0.20 cm^2, respectively.

Subsequent Ni depositions on these PPy films showed that for low anodic current densities, either no Ni deposition or large, irregularly shaped Ni deposits were observed by field-emission SEM. Consistent Ni growth was seen only when the anodic current density was sufficiently high to produce an end-point voltage near 2 V. A fairly high current density of 16 mA/cm^2 was therefore chosen for the PPy electrodeposition in the following Ni depositions.

The lack of uniform Ni nanoparticle deposition for PPy substrates grown at low current densities indicates that these PPy substrates have either significantly different conductivity or electric field homogeneity from those PPy substrates obtained at high current densities. In a study of PPy grown from a propylene carbonate solution, West et al. [9] found that the low current density form of PPy should be more highly conjugated and therefore have a higher capacity to accommodate more ClO_4^- dopant ions per pyrrole unit. One might expect a more conductive PPy layer to be more favourable for the growth of small sized, mono-dispersed Ni nanoparticles. We did not observe this, likely because the PPy film when grown at low current densities could also be less electrically homogeneous. More recent AFM studies by Lee and Park [12] indicated inhomogeneous electrical conductivity on the sub-micron scale in under-doped PPy films. Similar inhomogeneity may also exist in more fully doped films, thus confirming our present observation.

Although nickel could be deposited consistently on PPy grown at a current density of 16 mA/cm^2, sometimes larger fibrous spheres of Ni with diameters ranging from 50–1500 nm while other times smaller Ni particles with diameters less than 20 nm were produced. We observed that the type of particles formed was correlated to how the gold layer on silicon was prepared before the PPy substrate was deposited. This is exemplified in Fig. 2, which shows two typical voltage transients at 16 mA/cm^2 for galvanostatic PPy electrodeposition. In particular, Fig. 2(a) shows a “one-step” PPy transient, where the voltage rises sharply to ~2 V, and further Ni electrodeposition produces larger, fibrous Ni spheres (shown in inset). On the other hand, Fig. 2(b) shows a “two-step” PPy transient, where further Ni electrodeposition produces the smaller Ni nanoparticles. We associate this variation in the PPy growth with the adhesion of the gold thin film to the supporting conducting silicon chip. Baking the silicon chips at 100 °C for 30 min removes residual moisture, improves gold adhesion to the silicon, and makes the undesirable “one-step” transient less likely.

Adhesion of the gold film onto the silicon support is important in controlling the PPy growth and electrical properties, and thus the

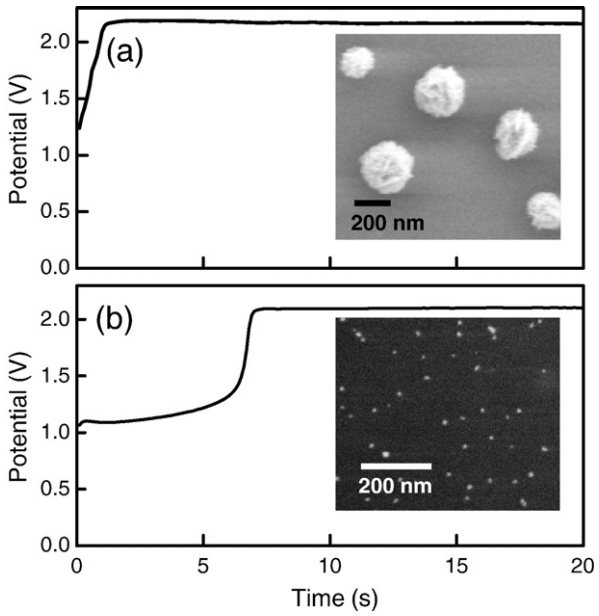

Fig. 2. Potential vs. time transient profiles during polypyrrole electrodeposition at a current density of 16 mA/cm^2. (a) A "one-step" transient is obtained for polypyrrole substrates that produce large, fibrous Ni nanoparticles. (b) A "two-step" transient is observed for polypyrrole substrates that produce small, well-dispersed Ni nanoparticles of 7–20 nm in diameter. The insets show scanning electron micrographs of the respective Ni nanoparticle morphologies.

subsequent Ni nanoparticle deposition. Earlier experiments [13] on PPy growth on Pt, Au and glassy carbon showed the importance of the substrate on the nucleation and growth of the PPy film. The present result therefore demonstrates how the PPy microstructure can affect the further growth of metallic nanoparticles.

3.2. Nickel nanoparticle growth

The smaller nanoparticles appearing as small bright spots in the SEM images (Fig. 2(b), inset) have been confirmed as nickel by in-situ Energy Dispersive X-ray (EDX) spot analysis. We examined some representative samples by TEM and XPS. As shown in Fig. 3(a), the TEM images indicate that these nanoparticles are 7 to 12 nm in diameter, and are ovoid structures without any obvious facetting. There are also some larger clusters of two or more nanoparticles. Dark-field TEM images indicate that the Ni nanoparticles appear as single crystals, while the clusters consist of a number of randomly oriented crystallites of 5–15 nm diameter. Further evidence of the crystalline structure of the Ni nanoparticles can be seen in the selected-area electron diffraction image, shown in Fig. 3(b). The observed ring spacings are characteristic of NiO (lattice spacing = 0.4177 nm), and not metallic nickel (lattice spacing = 0.3534 nm). This is not unexpected, because the nanoparticles were exposed to air after growth, and our earlier work on copper nanoparticles [7] also showed a copper oxide shell around a metallic copper core. Studies by Karmhag et al. [14] and Uchikoshi et al. [15] on metallic Ni nanoparticles with a similar size (20 nm) have also shown that a nickel oxide layer between 2 and 3 nm thick would form almost immediately upon exposure to air.

The presence of nickel oxide is confirmed by the corresponding XPS spectrum shown in Fig. 3(c). The sample exhibited a Ni $2p_{3/2}$ peak at 856 eV binding energy, which could be attributed to $Ni(OH)_2$, Ni_2O_3, or $NiO(OH)_2$ [16]. Depth-profiling by argon sputtering of the surface led to a peak shift to 854 eV, characteristic of Ni $2p_{3/2}$ in NiO [17], in good accord with our TEM diffraction data. Further sputtering produced no further shifts in the peak position, just the eventual decrease and disappearance of the Ni features as the nickel was removed. It should be noted that the discernibly small intensity of the Ni $2p_{3/2}$ peak at 852.8 eV, corresponding to metallic Ni, indicates that the metallic core represents only a minor component.

In order to determine the optimal conditions for producing small, well-dispersed Ni core-shell nanoparticles, we varied several parameters including the PPy film thickness, and the applied potential and total charge transfer during Ni deposition. Uniformly sized and well-distributed small Ni nanoparticles were found when the PPy film thickness was kept in the narrow range of 90–110 nm. If the PPy film was much thinner than 90 nm, no Ni particles could be observed by SEM. As the PPy film became thicker than 110 nm, the Ni particles also became more and more inhomogeneously distributed and sized.

By running cyclic voltammetric scans on PPy films in both the nickel solution and the corresponding nickel-free electrolyte solution, it was determined that the nickel was first reduced at a potential of −1.0 V. The voltage applied during the potentiostatic Ni deposition (with respect to a Ag/AgCl reference electrode) was varied between −1.0 V and −1.8 V, while the total charge transfer was kept constant at 1.9 mC. At −1.0 V and −1.2 V, occasional Ni nanoparticles were observed on the PPy film, but the total amount of Ni deposited was very small. Between −1.3 V and −1.6 V, well-distributed, uniformly sized Ni nanoparticles were observed. At −1.8 V, the Ni nanoparticles tended to cluster, and became irregularly sized and shaped. As the potential was varied, the total amount of Ni deposited on the film surface was also found to change, despite a constant total charge transfer was maintained. This occurred because hydrogen evolution could also contribute to the total charge transfer during the Ni deposition [1].

Nickel core-shell nanoparticles were also grown at a constant voltage of −1.4 V, while the total charge transfer was varied. Fig. 4

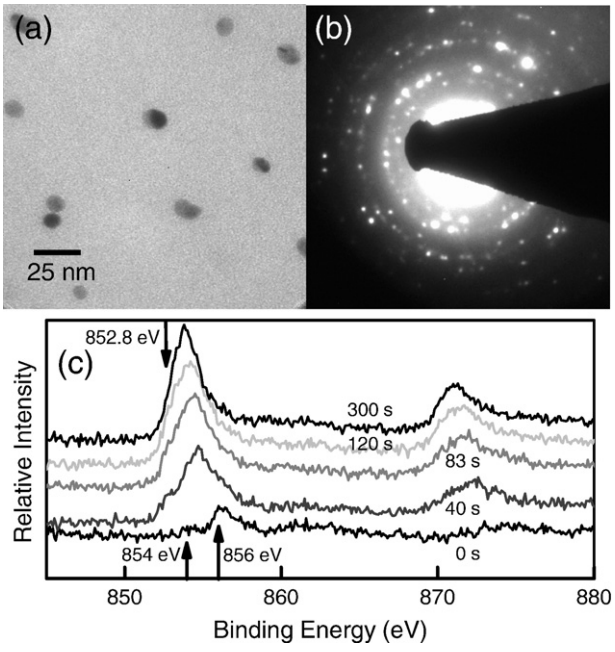

Fig. 3. (a) Transmission electron micrograph of the nickel nanoparticles taken at 200 kV, and (b) the corresponding electron diffraction image depicting the crystalline nature of the particles. (c) X-ray photoemission spectrum of the Ni 2p region before and after sequential sputtering for the indicated total sputtering time.

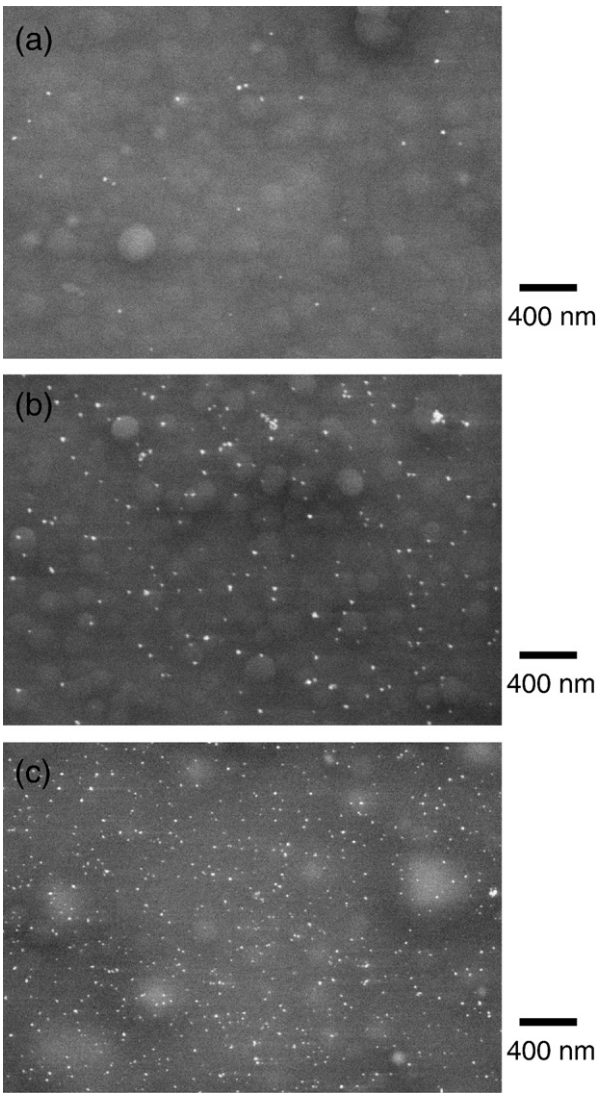

Fig. 4. SEM micrographs taken at 5 kV, depicting the increase in the number density of the Ni nanoparticles deposited at −1.4 V with increasing total charge transfer from (a) 1.9 mC, to (b) 2.6 mC, and (c) 3.2 mC.

shows the SEM images of the Ni nanoparticles deposited on PPy on the gold-coated silicon electrode for total charge transfers of (a) 1.9 mC, (b) 2.6 mC, and (c) 3.2 mC. At this voltage, as the total charge transfer was increased, the number density of the nanoparticles was found to increase correspondingly, without any significant change in the size of the nanoparticles. This type of growth is interesting because it is characteristic of progressive nucleation and growth, instead of the more commonly observed instantaneous nucleation [8]. While it would be necessary to deconvolute this from the effects of hydrogen evolution, it would be interesting to investigate in more detail the nickel nanocrystal growth mechanism in future work.

4. Conclusions

Conditions for growing uniformly sized and dispersed Ni core-shell nanoparticles (close to the quantum size regime) on PPy by electrodeposition have been determined. The amount and type of the deposited Ni nanoparticles critically depend on the preparation of the conducting polymer (PPy) substrate. A 90–110 nm thick PPy film grown at current densities at or above 16 mA/cm^2 on baked gold-coated silicon electrodes was found to facilitate reproducible deposition of Ni nanoparticles of ~10 nm in diameter, i.e. near the optimal size regime for such applications as nanocatalysis and quantum electronics. By manipulating the nature of the PPy substrate, it is therefore possible to selectively produce one of two types of nanoparticle morphologies: small Ni nanocrystallites ranging in diameter from 7 to 12 nm, and larger spherical Ni clusters, ranging in diameter from 100 nm to over a micron.

Acknowledgement

This work was supported by the Natural Sciences and Engineering Research Council of Canada.

References

[1] M.P. Zach, R.M. Penner, Adv. Mater. 12 (2000) 878–883.
[2] U. Heiz, F. Vanolli, A. Sanchez, W.D. Schneider, J. Am. Chem. Soc. 120 (1998) 1668.
[3] N. Takano, D. Niwa, T. Yamada, T. Osaka, Electrochim. Acta 45 (2000) 3263.
[4] P. Zhang, F. Zuo, F.K. Urban III, A. Khabari, P. Griffiths, A. Hosseini-Tehrani, J. Magn. Magn. Mater. 225 (2001) 337.
[5] M.T. Reetz, W. Helbig, J. Am. Chem. Soc. 116 (1994) 7401.
[6] F. Fiévet, J.-P. Lagier, M. Fietglarz, MRS Bull. 14 (1989) 29.
[7] X.J. Zhou, A.J. Harmer, N.F. Heinig, K.T. Leung, Langmuir 20 (2004) 5109.
[8] D.K. Sarkar, X.J. Zhou, A. Tannous, K.T. Leung, J. Phys. Chem. B 107 (2003) 2879.
[9] K. West, T. Jacobsen, B. Zachau-Cristiansen, Synth. Met. 55/57 (1993) 1412.
[10] S. Asavapiriyanont, G.K. Chandler, G.A. Gunawardena, D. Pletcher, J. Electroanal. Chem. 177 (1984) 229.
[11] G. Paasch, D. Schmeisser, A. Bartl, H. Naarmann, L. Dunsch, W. Goepel, Synth. Met. 66 (1994) 135.
[12] H.J. Lee, S.M. Park, J. Phys. Chem. B 108 (2004) 1590.
[13] M.F. Suárez, R.G. Compton, J. Electroanal. Chem. 462 (1999) 211.
[14] R. Karmhag, G.A. Niklasson, M. Nygren, J. Appl. Phys. 89 (2001) 3012.
[15] T. Uchikoshi, Y. Sakka, M. Yoshitake, K. Yoshihara, Nanostruct. Mater. 4 (1994) 199.
[16] K.S. Kim, N. Winograd, Surf. Sci. 43 (1974) 625.
[17] J.F. Moulder, W.F. Stickle, P.E. Sobol, K.D. Bomben, Handbook of X-Ray Photoelectron Spectroscopy, Perkin-Elmer, 1992.
[18] A. Lachenwitzer, O.M. Magnussen, J. Phys. Chem. B 104 (2000) 7424.